

The effect of Th substitution and of magnetic field on Kondo semiconducting behaviour in
 U_2Ru_2Sn

This article has been downloaded from IOPscience. Please scroll down to see the full text article.

2001 J. Phys.: Condens. Matter 13 8375

(<http://iopscience.iop.org/0953-8984/13/36/311>)

View [the table of contents for this issue](#), or go to the [journal homepage](#) for more

Download details:

IP Address: 171.66.16.226

The article was downloaded on 16/05/2010 at 14:50

Please note that [terms and conditions apply](#).

The effect of Th substitution and of magnetic field on Kondo semiconducting behaviour in U_2Ru_2Sn

P de V du Plessis¹, A M Strydom², R Troć³ and L Menon¹

¹ f-Electron Magnetism and Heavy-Fermion Physics Research Programme, School of Physics, University of the Witwatersrand, Private Bag 3, PO Wits 2050, Johannesburg, South Africa

² Physics Department, Rand Afrikaans University, PO Box 524, Auckland Park 2006, Johannesburg, South Africa

³ W Trzebiatowski Institute for Low Temperature and Structure Research, Polish Academy of Sciences, PO Box 1410, 50-950 Wrocław 2, Poland

E-mail: ams@na.rau.ac.za (A M Strydom)

Received 26 June 2001

Published 23 August 2001

Online at stacks.iop.org/JPhysCM/13/8375

Abstract

Electrical resistivity, $\rho(T)$, measurements on U_2Ru_2Sn show typical Kondo semiconducting behaviour, namely a $\rho(T) \sim \ln T$ behaviour at higher temperatures and an activation-like increase in $\rho(T)$ below 20 K which indicates the opening of a small gap in the electronic density of states. The magnetic susceptibility, $\chi(T)$, of U_2Ru_2Sn has a maximum around 180 K which is characteristic of intermediate-valence behaviour. The $\chi(T)$ data for U_2Ru_2Sn have been fitted to the interconfigurational fluctuation model of Sales and Wohllleben giving a value of $T_{sf}^* = 155(2)$ K for the characteristic fluctuation temperature. Substituting as little as 5% Th for U leads to a $\rho(T)$ variation reminiscent of that of a single-ion Kondo metal $\rho(T) = \rho(0)[1 - (\pi^2/16)(T^2/T_K^2)]$. Values of $T_K = 79(1)$ and $113(1)$ K are respectively obtained for alloys with 5% and 10% Th substitution.

1. Introduction

A number of f-electron compounds show semiconducting behaviour at low temperatures with an activation type of increase of the resistivity upon lowering the temperature. These materials have been referred to in the literature either as Kondo insulators [1] or as heavy-fermion semiconductors [2]. It is thought that a gap opens in the Fermi surface because of hybridization of the conduction electrons with the nearly localized f electrons [1]. The magnitude of the hybridization gap Δ/k_B (k_B is Boltzmann's constant) ranges for example from 3500 K in TmTe, to 1200 K for $U_3Ni_3Sb_4$, to 42 K for $Ce_3Bi_4Pt_3$ and to as low as 3 K for CeNiSn. For a more complete compilation for other strongly correlated rare-earth or uranium semiconductor systems, reference should be made to review papers by Aeppli and Fisk [1] and Riseborough [2].

The rare-earth-based Kondo semiconductors are often not magnetically ordered: their susceptibility, $\chi(T)$, in many instances follows a Curie–Weiss behaviour at high temperature with effective magnetic moments close to the values expected for the trivalent Ce or Yb ions (e.g. $\text{Ce}_3\text{Bi}_4\text{Pt}_3$ [1, 3], CeNiSn [4], YbB_{12} [4]). At lower temperatures a broad maximum appears in the $\chi(T)$ curves of many Kondo semiconductors: for example at temperatures T_{max} of 75 K, 80 K and 125 K for YbB_{12} [4], $\text{Ce}_3\text{Bi}_4\text{Pt}_3$ [5] and CeRhSb [6] respectively. Values of $T_{\text{max}} \sim 100$ K and higher are characteristic of intermediate-valence (IV) behaviour [7]. For Ce compounds the Kondo temperature $T_K \sim 3 T_{\text{max}}$ [8]. The appearance of a broad maximum in $\chi(T)$ of CeRhSb has been analysed [6, 9] in terms of IV behaviour by using either the interconfiguration (ICF) model of Sales and Wohleben [10] or the Bethe-*ansatz* solution of the Coqblin–Schrieffer Hamiltonian as given by Rajan [11]. In a few cases magnetic order has been found in some Kondo semiconductor systems; e.g. TmSe [12], TmTe [13] and UNiSn [14] are antiferromagnetic below $T_N = 6.5$ K, 0.4 K and 47 K respectively, while $\text{UFe}_4\text{P}_{12}$ is a ferromagnet below $T_C = 3.1$ K [15]. In the case of UNiSn , the paramagnetic \rightarrow antiferromagnetic transition is accompanied by a transition to metallic behaviour at T_N and consequently the material is semiconducting only at higher temperatures.

The resistivity $\rho(T)$ of Kondo semiconductors shows two kinds of behaviour. Materials belonging to the first group (e.g. $\text{Ce}_3\text{Bi}_4\text{Pt}_3$ [5], and YbB_{12} [4]) exhibit an activation type of increase $\rho(T) \propto \exp(\Delta/k_B T)$ with decreasing temperature which is then usually followed by extrinsic behaviour at the lowest temperatures. The behaviour of the second group of materials is more complicated. With decreasing temperature $\rho(T)$ first increases, then goes through a maximum which at lower temperature is followed by a minimum before it finally increases again towards the lowest temperature due to the opening of a gap. Examples of such behaviour are found in CeRhSb [6, 9, 16] and CeNiSn [16]. It has been observed in single-crystal studies of CeRhSb and CeNiSn that the magnitude of this low-temperature increase in $\rho(T)$, and hence the size of the gap Δ , is greatly reduced as sample purity is increased [16]. For orthorhombic CeNiSn for which the gap formation is anisotropic [17], the *a*-axis resistivity of the purest samples becomes independent of temperature below 1.5 K. This suggests that the gap collapses in this direction and consequently this material develops gapless excitations within a hybridization pseudogap [18, 19]. Theoretical models describing gap formation are referred to in a recent review paper [2]. Significant changes in transport and other properties of Kondo semiconducting materials are obtained by diluting the cerium or uranium compound with La [5, 6, 9], or Th [20, 21] or by doping with transition elements [16, 22].

Magnetoresistance measurements have been reported for CeNiSn [14, 16], CeRhSb [23] and $\text{Ce}_3\text{Bi}_4\text{Pt}_3$ [24]. A 25% reduction of the gap in CeNiSn was observed upon application of a magnetic field of 5.8 T [25]. For YbB_{12} transport measurements indicate that the application of a field of 55 T completely suppressed the gap resulting in an insulator–metal transition [26]. Furthermore, measurements of the specific heat of $\text{Ce}_3\text{Bi}_4\text{Pt}_3$ in magnetic fields up to 60 T indicate closure of the gap by such a magnetic field [27]. A theoretical description of the closure of the energy gap and the accompanying insulator–metal transition in Kondo insulators has been given by Saso and Itoh [28].

The present paper is concerned with the results of resistivity, magnetic susceptibility and magnetoresistivity measurements performed on several $(\text{U}_{1-x}\text{Th}_x)_2\text{Ru}_2\text{Sn}$ alloys. In an earlier paper [29] we reported on resistivity measurements (4–300 K) on the parent compound $\text{U}_2\text{Ru}_2\text{Sn}$ and showed that its $\rho(T)$ is characteristic of the second kind of behaviour associated with Kondo semiconductors as described in section 1. Now we present the results of extending our $\rho(T)$ measurements down to 1.4 K. We furthermore report on the magnetoresistance (MR) measured in fields up to 8 T and the temperature dependence of the susceptibility between

1.7 K and 400 K. These studies are performed for both the parent compound U_2Ru_2Sn and several alloys formed by replacing U with Th in this compound.

2. Experimental details

The samples were prepared by melting the constituents in an arc furnace under a titanium-gettered atmosphere of ultrahigh-purity argon. Two sets of samples were studied, namely samples prepared using higher-purity Ru (99.99 wt%) and samples prepared using Ru of purity 99.9 wt%. The purities of other elements used are as follows: U(99.98 wt%), Th(99.99 wt%) and Sn(99.999 wt%). Negligible weight loss occurred during the arc-melting of the samples. Room temperature x-ray diffraction patterns of all the alloys studied could be indexed according to the ordered version of the tetragonal U_3Si_2 type of structure ($P4/mbm$). The observed x-ray patterns showed no evidence for the existence of any parasitic phases. Lattice parameters, as determined by means of x-ray diffraction, are given in table 1 and values for the parent compound U_2Ru_2Sn are in reasonable agreement with those given by Mirambet *et al* [30].

Table 1. Lattice parameters at room temperature of $(U_{1-x}Th_x)_2Ru_2Sn$ alloys.

x	a (Å)	c (Å)	V (Å ³)
0	7.500(1)	3.563(1)	200.4(1)
0.05	7.505(3)	3.573(2)	201.2(3)
0.1	7.512(2)	3.593(2)	204.8(6)
0.2	7.529(6)	3.613(4)	204.8(6)
0	7.486(2)	3.558(1)	199.3(2)
Reference [30]			

Electrical resistivity and MR measurements were performed on bar-shaped samples ($1 \times 1 \times 8$ mm³) which were cut by spark-erosion from the sample ingots. The four-probe dc method was used with contact wires spot-welded onto the specimens. A current-reversal procedure was employed to counter possible thermal voltages in the circuitry. A YEW-type 2854 dc source provided constant current through our samples and voltages were measured using a HP 3478A digital voltmeter. Initial transport measurements were performed in the temperature range 4–300 K. Temperatures were measured using a Au–0.07 at.% Fe versus chromel thermocouple. In subsequent work temperatures down to 1.4 K were attained using an Oxford Instruments variable-temperature insert in conjunction with a superinsulated Dewar and a superconducting solenoid provided fields up to 8 T. Sample temperatures were regulated using an Oxford Instruments ITC⁵⁰³ temperature controller and measured by means of calibrated resistive carbon-glass and germanium sensors. During MR measurements a magnetic-field-insensitive capacitance sensor provided input to the temperature controller.

DC magnetization measurements were performed on solid pieces of sample using a Quantum Design MPMS-5 SQUID magnetometer. Applied magnetic fields up to 5 T and temperatures in the range 1.7–400 K were used.

3. Results and discussion

The temperature dependences of the resistivity $\rho(T)$ for alloys in the series $(U_{1-x}Th_x)_2Ru_2Sn$ are shown in figure 1 and figure 2 for samples prepared using Ru of higher-purity (labelled I) and of lesser purity (labelled II). Both the U_2Ru_2Sn (I) and U_2Ru_2Sn (II) samples exhibit characteristics typical of the materials that belong to the second group of Kondo semiconductors

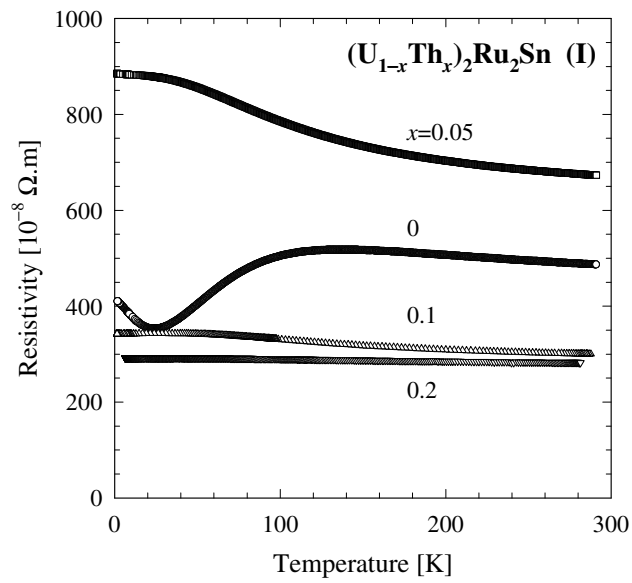


Figure 1. The temperature dependence of the electrical resistivity of $(U_{1-x}Th_x)_2Ru_2Sn$ alloys synthesized using higher-purity Ru (99.99 wt%). These alloys are designated $(U_{1-x}Th_x)Ru_2Sn$ (I) throughout the paper.

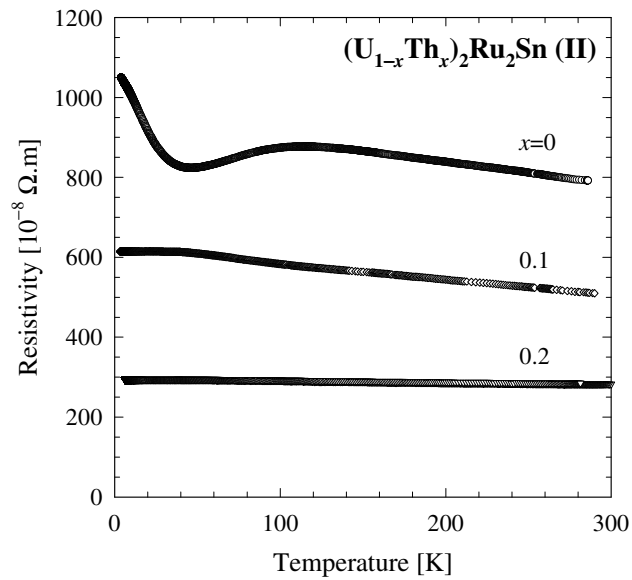


Figure 2. The temperature dependence of the electrical resistivity of $(U_{1-x}Th_x)_2Ru_2Sn$ alloys synthesized using less pure Ru (99.9 wt%). These alloys are designated as $(U_{1-x}Th_x)_2Ru_2Sn$ (II).

as described in section 1. Below room temperature, the resistivity increases with decrease in temperature for both U_2Ru_2Sn (I) and U_2Ru_2Sn (II) samples, until a broad maximum is observed near 130 K for U_2Ru_2Sn (I) and near 120 K for U_2Ru_2Sn (II). Upon further cooling, $\rho(T)$ decreases for both samples; this is followed by a minimum at about 25 K for U_2Ru_2Sn

(I) and near 40 K for the U₂Ru₂Sn (II) sample. Finally, below this minimum $\rho(T)$ increases for both samples. The rise in resistivity at low temperatures is smaller for the higher-purity U₂Ru₂Sn (I) sample than for the U₂Ru₂Sn (II) sample. This agrees with similar findings for CeNiSn and CeRhSb samples [16] as discussed in section 1.

In figure 1 it is shown that a small 5% Th doping completely destroys the typical Kondo insulator characteristics and leads to a $\rho(T)$ variation that is reminiscent of the behaviour of a single-ion Kondo metal. The magnitude of this single-ion Kondo resistivity decreases rapidly with further Th doping. We note that the results presented in figure 1 and figure 2 show similar qualitative features, but the resistivity values are generally higher for the (U_{1-x}Th_x)₂Ru₂Sn (II) alloys than for the (U_{1-x}Th_x)₂Ru₂Sn (I) alloys.

In the following we will present and discuss data that pertain only to the (U_{1-x}Th_x)₂Ru₂Sn (I) samples. Results of the magnetic susceptibility measurements are given in figure 3. These relate to measurements in applied fields of 5 T since it was observed that the magnetization versus field isotherms are linear up to this field for all the alloy compositions studied. The $\chi(T)$ results for the U₂Ru₂Sn (I) sample are characteristic of fluctuating-valence materials. The broad maximum in $\chi(T)$ at around 180 K for U₂Ru₂Sn (I) is weakened with 5% Th doping and is no longer seen for the $x = 0.1$ alloy. The $x = 0.1$ alloy and especially the $x = 0.2$ alloy exhibit a sharp upturn in $\chi(T)$ towards low temperatures.

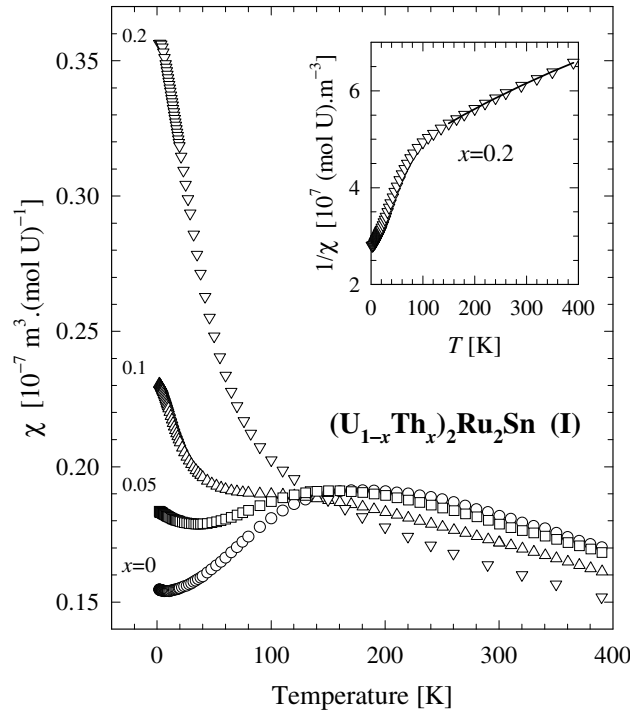


Figure 3. The temperature dependence of the magnetic susceptibility $\chi(T)$ of (U_{1-x}Th_x)₂Ru₂Sn (I) alloys. Intermediate-valence behaviour is observed for the parent compound U₂Ru₂Sn (I).

In the inset to figure 3 it is shown by a solid line that for a temperature range 140–390 K the $\chi(T)$ data for the $x = 0.2$ alloy fit a modified Curie–Weiss law

$$\chi(T) = \chi_0 + \frac{N_A \mu_{\text{eff}}^2}{3k_B(T - \theta_p)} \quad (1)$$

where N_A is Avogadro's number and k_B is Boltzmann's constant. The following least-squares-fit values were obtained: $\chi_0 = 9.4(1) \times 10^{-9} \text{ m}^3 (\text{mol U})^{-1}$, $\mu_{\text{eff}} = 1.5(1) \mu_B (\text{mol U})^{-1}$ and $\theta_p = 239(10) \text{ K}$. The sharp upturn in the $\chi(T)$ curve and associated sharp downturn in the $\chi^{-1}(T)$ curve below 100 K is similar to the behaviour of $\text{U}_2\text{Rh}_2\text{In}$ [31].

The $\chi(T)$ behaviour for $\text{U}_2\text{Ru}_2\text{Sn}$ (I) is reminiscent of that of several Ce IV compounds like CeSn_3 [32], CeRhSb [6, 9], $\text{Ce}_2\text{Ni}_2\text{In}$ [33] and $\text{Ce}_2\text{Rh}_2\text{In}$ [33]. A description of the $\chi(T)$ dependence of these Ce compounds has been given in terms of two IV models, namely the paramagnon model of Beál-Monod and Lawrence [32] valid at lower temperatures and the ICF fluctuation model of Sales and Wohlleben [10]. These models will be used to describe $\chi(T)$ of $\text{U}_2\text{Ru}_2\text{Sn}$ although one is aware that the valence fluctuations are likely to be between two magnetic states for U compounds [35] rather than between a magnetic and a non-magnetic state as for Ce compounds [10, 34]. However, considering the uncertainty of the electronic structure of U compounds in general and for $\text{U}_2\text{Ru}_2\text{Sn}$ in particular, and the lack of an appropriate theory of IV behaviour of actinide compounds, we investigate in the following to what extent the above theories describe the $\chi(T)$ results for $\text{U}_2\text{Ru}_2\text{Sn}$ (I).

The T^2 -like behaviour of $\chi(T)$ of $\text{U}_2\text{Ru}_2\text{Sn}$ (I) seen in figure 3 at low temperatures may be described in terms of the paramagnon model. However, the small upturn in $\chi(T)$ observed at the lowest temperatures cannot be described by this model and for Ce compounds a similar upturn has been regarded as an impurity effect showing a Curie-like temperature dependence [32, 34]. The expected $\chi(T)$ behaviour at low temperature is hence given as

$$\chi(T) = \chi(0) + \frac{C^{\text{imp}}}{T} + b \frac{T^2}{T_{\text{sf}}^2}. \quad (2)$$

$\chi(0)$ is the intrinsic susceptibility of the IV compound at $T = 0 \text{ K}$, the second term refers to the impurity contribution and the third term is the paramagnon contribution. T_{sf} denotes a characteristic temperature for spin fluctuations and the constant b is of the order of unity. We show a fit of the experimental $\chi(T)$ data to (2) for the temperature interval $1.7 \leq T \leq 40 \text{ K}$ in figure 4 by means of a dashed line. The fit parameters $\chi(0)$, C^{imp} and T_{sf} (with b taken as 1) are given in table 2.

Table 2. Fit parameters for the susceptibility $\chi(T)$ of $\text{U}_2\text{Ru}_2\text{Sn}$ (I) for intermediate-valence models (see figure 4).

	Paramagnon model, equation (2), curve 1	ICF model, equations (3) and (4)		
			Curve 2	Curve 3
$\chi(T)$	$0.153(1) \text{ m}^3 (\text{mol U})^{-1}$	μ_{eff}	$4.40(1) \mu_B$	$3.58(1) \mu_B$
C_{imp}	$0.0025(3) \text{ m}^3 (\text{mol U})^{-1} \text{ K}$	T_{sf}^*	$155(2) \text{ K}$	$40(5) \text{ K}$
b	$1 \text{ m}^3 (\text{mol U})^{-1}$	$\Delta E/k_B$	$-349(2) \text{ K}$	$-230(2) \text{ K}$
T_{sf}	$515(1) \text{ K}$	J	4	4

For temperatures above 60 K we fitted the data for the $\text{U}_2\text{Ru}_2\text{Sn}$ (I) sample in accordance with the ICF model of Sales and Wohlleben [10]. In their formulation the valence fluctuations are considered to take place between a magnetic state of effective moment μ_{eff} and total angular momentum J and a non-magnetic state. The susceptibility is then given by

$$\chi(T) = \frac{N\mu_{\text{eff}}^2[1 - \nu(T)]}{3k_B(T + T_{\text{sf}}^*)} \quad (3)$$

and the fractional occupation of the non-magnetic state is given by

$$\nu(T) = \left\{ 1 + (2J + 1) \exp \left[-\Delta E/k_B(T + T_{\text{sf}}^*) \right] \right\}^{-1}. \quad (4)$$

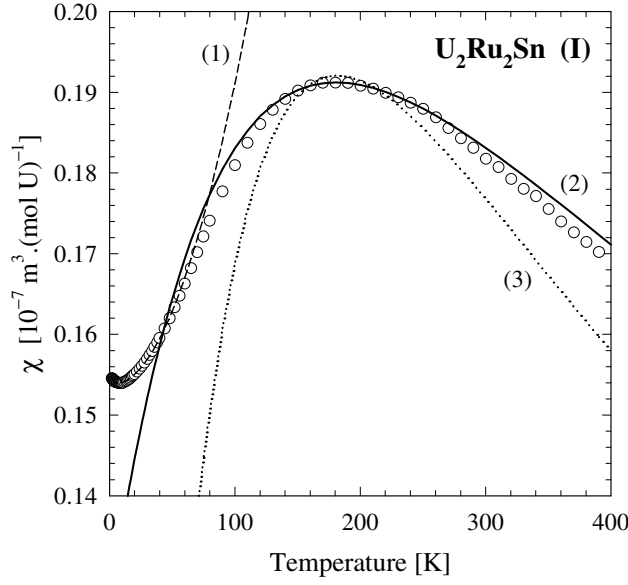


Figure 4. The temperature dependence of the susceptibility of U₂Ru₂Sn (I) is fitted for curve (1) to the paramagnon model of Béal-Monod and Lawrence and for curves (2) and (3) to the interconfiguration fluctuation model of Sales and Wohlleben. Parameters pertaining to these fits and the physical significance of these are given in table 2 and discussed in the text.

The characteristic temperature associated with fluctuations between the two states is given by T_{sf}^* and the states are separated by ΔE . In figure 4 we show as a solid line a least-squares fit of $\chi(T)$ for U₂Ru₂Sn (I) against (3) and (4). Using $J = 4$ we obtain the fit parameters μ_{eff} , T_{sf}^* and ΔE as given in table 2. The valence changes monotonically from 3.99 at 1.4 K to 3.94 at 400 K. The values of T_{sf}^* and T_{sf} obtained using the two different models agree within the order-of-unity value that b takes in the paramagnon model. The value of $\mu_{eff} = 4.4\mu_B$ obtained from the solid-line fit is larger than that corresponding to either a U⁴⁺ 5f² or a U³⁺ 5f³ free-ion configuration, namely 3.58 or 3.62 μ_B . We illustrate by means of a dotted line in figure 4 that using a smaller value $\mu_{eff} = 3.58\mu_B$ and $J = 4$ in (3) and (4) gives an unsatisfactory fit of the experimental data. The possible meaning of these results will be discussed in section 4.

In figure 5 it is illustrated with a solid line that the $\rho(T)$ data of U₂Ru₂Sn (I) at high temperature are characteristic of incoherent Kondo scattering:

$$\rho(T) = \rho_0 - \rho_K \ln T. \quad (5)$$

The fit parameters ρ_0 and ρ_K are given in table 3. The low-temperature rise in $\rho(T)$ below 25 K is fitted to an activation-type temperature dependence characteristic of a Kondo semiconductor:

$$\rho(T) = c \exp(\Delta/k_B T). \quad (6)$$

In (6), Δ is the energy gap, k_B is Boltzmann's constant and c is a variable coefficient. A plot of $\ln \rho$ versus $1/T$ is given in the inset to figure 5. It is observed that an activation behaviour is followed only in the temperature range 11–17 K as indicated by a solid line in the inset with fit parameters given in table 3. At lower temperatures the data deviate from an activated behaviour. Such a deviation has been observed for several other Kondo semiconducting materials, e.g. YbB₁₂ [36,37], CeRhAs [38], CeNiSn [39] and CeRhSb [9,23] and Ce₃Bi₄Pt₃ under pressure [24]. In fact in most of these studies [9,36–39] the $\ln \rho$ versus $1/T$ curves are interpreted as exhibiting two linear regions, one at higher temperature and one

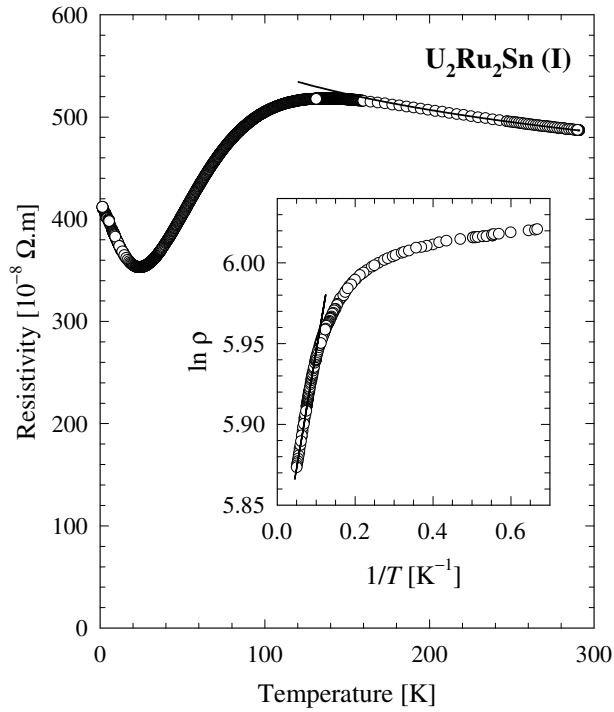


Figure 5. The electrical resistivity $\rho(T)$ of $\text{U}_2\text{Ru}_2\text{Sn}$ (I) is given in the main figure. At higher temperatures an incoherent Kondo $\rho(T) \sim -\ln T$ behaviour is found as indicated by a solid line. A 1:5 depopulated data set is shown for $T \geq 160$ K in order to show the fit. The data follow a thermally activated temperature dependence between 11 and 17 K as indicated by a solid line in the inset.

Table 3. Fit parameters for $\text{U}_2\text{Ru}_2\text{Sn}$ (I) and $\text{U}_{1-x}\text{Th}_x\text{Ru}_2\text{Sn}$ (I) alloys describing the electrical transport.

x	Equation (5)		Equation (6)		Equation (7)	
	ρ_0 (10^{-8} Ω m)	ρ_K (10^{-8} Ω m)	c (10^{-8} Ω m)	Δ/k_B (K)	$\rho(0)$ (10^{-8} Ω m)	T_K (K)
$\text{U}_2\text{Ru}_2\text{Sn}$ (I) (zero field)	586(5)	53.8(6)	331(1)	1.43(1)		
0.05 (zero field)	1284(2)	109(1)			883(1)	79(1)
0.10 (zero field)	460(1)	28.4(2)			346(1)	113(1)
$\text{U}_2\text{Ru}_2\text{Sn}$ (I) ($B = 8$ T)			344(1)	2.26(4)		

at low temperatures. The behaviour at low temperatures has been considered as of extrinsic origin [36]. For our data the temperature range for which a possible linear $\ln \rho$ versus $1/T$ is observed at low temperatures is less than 1 K. Hence we do not ascribe an activated behaviour to the resistivity at the lowest temperatures. For the Kondo semiconductor $\text{Ce}_3\text{Bi}_4\text{Pt}_3$, its low-temperature $\rho(T)$ has been described in terms of a variable-range hopping mechanism

$\rho(T) \sim \exp[(T_0/T)^{1/4}]$. Also for IV PuTe [41], a Mott's law variable hopping conductivity $\sigma \sim \exp[-(T_0/T)^{1/4}]$ is invoked to describe its low-temperature behaviour [42]. We tested our experimental data for this temperature dependence, but found that they do not conform to such a description at all.

The value $\Delta/k_B = 1.43$ K observed for the energy gap of U₂Ru₂Sn (I) is small and comparable to that observed for CeNiSn [1, 16, 17]. An analysis of the data of figure 2 for the less pure U₂Ru₂Sn (II) sample gives results that are qualitatively similar to those observed for U₂Ru₂Sn (I), but with a Δ/k_B value approximately two times larger than for the higher-purity sample. Studies on the Kondo semiconductor materials CeNiSn and CeRhSb also indicate that the low-temperature increase in resistivity for higher-purity samples is smaller than for less pure materials [16].

Results of $\rho(T)$ for the alloys (U_{1-x}Th_x)₂Ru₂Sn (I) with $x = 0.05$ and 0.1 are depicted in figure 6. At high temperatures, $\rho(T)$ also follows the Kondo-like behaviour of (5) and the parameters of the least-squares fit of the data to this equation are included in table 3. The results indicate the single-ion Kondo character of the resistivity for these two alloys. The renormalization group treatment of the single-impurity Anderson model by Krishna-murthy *et al* [43] was extended by Sakai *et al* [44, 45] and leads to the following low-temperature ($T < 0.1 T_K$) expression for the resistivity:

$$\rho(T) = \rho(0) \left[1 - \frac{\pi^4 T^2}{16 T_K^2} \right]. \quad (7)$$

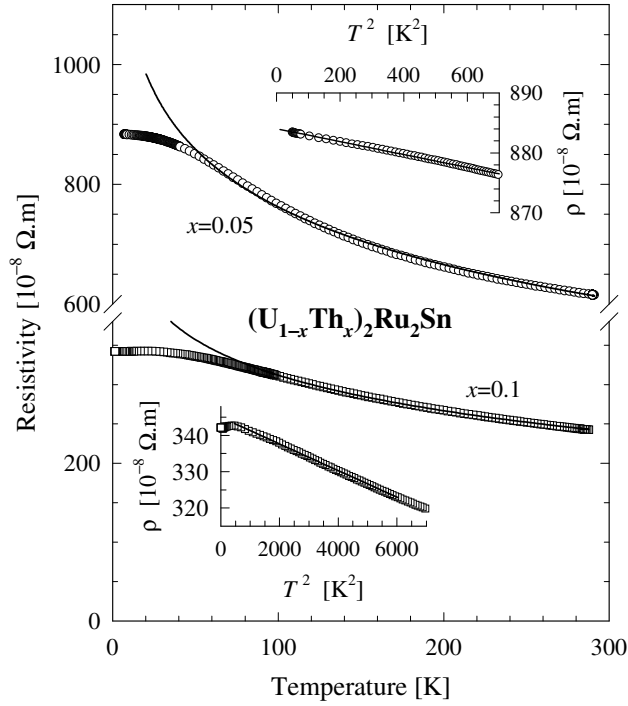


Figure 6. The electrical resistivities $\rho(T)$ of the (U_{1-x}Th_x)₂Ru₂Sn (I) alloys ($x = 0.05, 0.1$) are displayed in the main figure and follow an incoherent Kondo $\rho(T) \sim -\ln T$ dependence at high temperature (solid lines). The inset figures illustrate a Fermi-liquid $\rho(T) \sim 1 - a(T/T_K)^2$ dependence.

This expression is also obtained in a phenomenological Fermi-liquid approach [46]. Least-squares fits of our results to (7) are indicated in the insets to figure 6. Apart from some structure in $\rho(T)$ at the lowest temperatures for the $x = 0.1$ alloy, reasonable fits to (7) are obtained. Values of T_K found from these fits are also given in table 3. These large values of $T_K \sim 100$ K suggest that intermediate-valence behaviour can be expected in these alloys.

Finally, the effect of the application of a magnetic field up to 8 T on the resistivity was investigated for the U_2Ru_2Sn (I) sample. In figure 7 results from isofield runs at 3.5 and 8 T are compared with the zero-field data for U_2Ru_2Sn (I). The quantity $\Delta\rho = \rho(T, B) - \rho(T, 0)$ is positive but the main features of the anomaly are the same. The minimum in resistivity shifts from 24 K in zero field to 30 K in 8 T. Above 60 K results from zero-field and 8 T isofield curves are indistinguishable. We show in the inset to figure 7 the effect of the 8 T field on the thermally activated resistivity increase by presenting a plot of $\ln \rho$ versus $1/T$. From this plot a value of $\Delta/k_B = 2.26$ K is obtained which is somewhat higher than what is observed in zero field. On both experimental and theoretical grounds it is expected that application of a magnetic field should rather lead to a reduction in the energy gap as discussed in section 1.

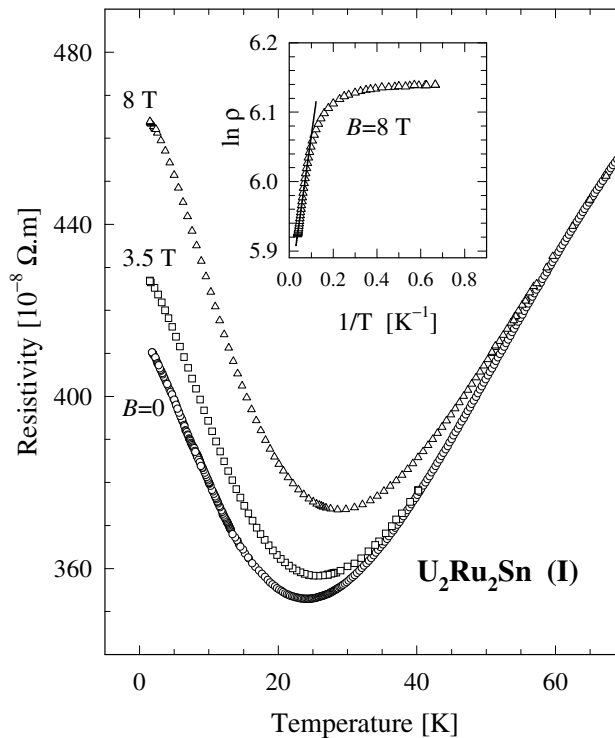


Figure 7. The temperature dependence of the resistivity $\rho(T)$ of U_2Ru_2Sn (I) measured for values of $B = 0, 3.5$ or 8 T. In the inset a plot of $\ln \rho$ versus $1/T$ for $B = 8$ T illustrates thermally activated behaviour (see table 3).

Measured values of $MR = \rho(T, B)/\rho(T, 0)$ for U_2Ru_2Sn (I) for fields up to 8 T are given for several isotherms in figure 8. Positive MR values up to 13% are obtained at 1.7 K. It is illustrated in the inset that in smaller fields ($B \leq 3$ T) the MR follows a power-law dependence $MR \sim B^n$ with n ranging between 1.85(2) for the 1.5 K isotherm and 2.05(2) for the 40 K isotherm. We note that a positive magnetoresistance has also been observed for the Kondo insulator compound $CeRhSb$ [23].

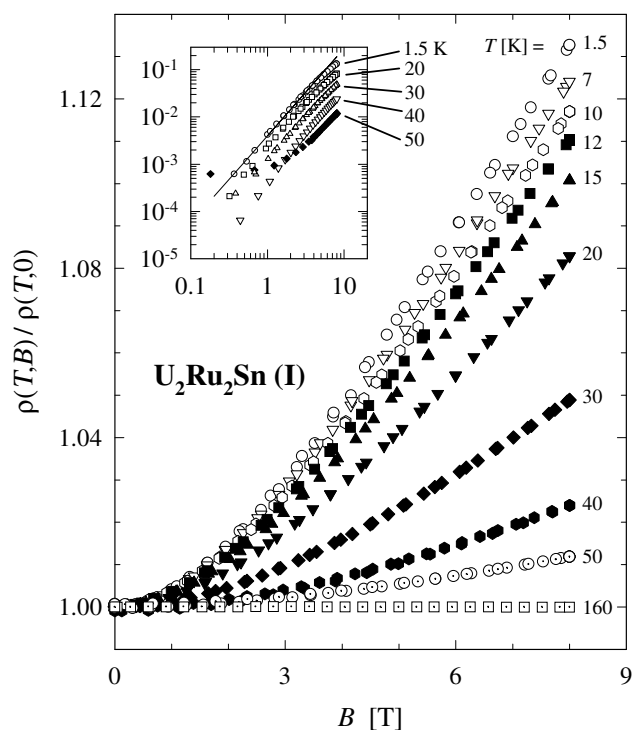


Figure 8. The magnetoresistance $MR = \rho(T, B)/\rho(T, 0)$ as a function of B for various isotherms. In the inset it is shown that the magnetoresistance follows a power law, $MR \sim B^n$.

4. Conclusions

The electrical resistivity $\rho(T)$ of U₂Ru₂Sn shows typical Kondo semiconducting behaviour. At higher temperatures $\rho(T) \sim \ln T$ as expected for incoherent Kondo scattering, while at low temperatures an activation-type temperature dependence is obtained indicating the opening of a small gap in the electronic density of states. A small degree of substitution of Th for U rapidly suppresses the semiconducting characteristics in U₂Ru₂Sn and leads to behaviour reminiscent of that of single-ion Kondo metals.

The susceptibility $\chi(T)$ of U₂Ru₂Sn exhibits the behaviour expected for fluctuating-valence materials and is described in terms of the paramagnon model of Béal-Monod and Lawrence and the interconfiguration fluctuation model of Sales and Wohlleben. It is indicated that a value of $\mu_{\text{eff}} = 4.4 \mu_B$ is required in order to obtain a good fit of our data against the ICF model. Such a value is considerably higher than the μ_{eff} -values associated with $5f^2$ or $5f^3$ electron configurations. A possible mechanism for obtaining such an enhanced μ_{eff} -value would be an electron configuration with a 6d contribution in addition to the 5f electrons. Such a configuration ($5f^{6-x}6d^x$) has been suggested for the Pu chalcogenides on the basis of band-structure calculations [47]. In analogy, the mixed-valence state in U₂Ru₂Sn may be realized by the hybridized $5f^{n-x}6d^x$ states with $n = 2$ or 3. One should furthermore be aware that the mixed-valence phenomenon in actinides is likely to be different from that in rare-earth compounds [35, 36], due *inter alia* to larger 5f spin-orbit coupling and 5f hybridization than the corresponding effects in rare-earth compounds. Therefore any conclusions regarding the electronic state of U₂Ru₂Sn should rather await appropriate spectroscopic studies.

The broad maximum in $\chi(T)$ near 180 K for $\text{U}_2\text{Ru}_2\text{Sn}$ which is characteristic of intermediate-valence behaviour is rapidly weakened with Th doping. The $x = 0.2$ alloy follows a modified Curie–Weiss relationship above 140 K and a somewhat anomalous behaviour at lower temperatures. To our knowledge $\text{U}_2\text{Ru}_2\text{Sn}$ is the first uranium compound to exhibit both the magnetic and electrical transport behaviours found in some well-studied Ce Kondo insulators: its $\chi(T)$ curve shows the intermediate-valence behaviour of the canonical Kondo insulator systems $\text{Ce}_3\text{Bi}_4\text{Pt}_3$ and CeRhSb while its $\rho(T)$ is reminiscent of the behaviour of CeNiSn and CeRhSb . The $\text{U}_2\text{Ru}_2\text{Sn}$ compound certainly warrants further studies of the effect of substitutions on its physical properties and also investigations employing other measuring techniques.

Acknowledgments

Financial support by the South African National Research Foundation and by the University of the Witwatersrand Research Committee is acknowledged. The work at the Institute for Low Temperature and Structure Research, Wrocław, was supported by the State Committee for Scientific Research in Poland within Grant No 2P03B 150 17. R Gorzelniak and D Badurski are thanked for valued technical assistance.

References

- [1] Aeppli G and Fisk Z 1992 *Comment. Condens. Matter Phys.* **16** 155
- [2] Riseborough P S 2000 *Adv. Phys.* **49** 257
- [3] Fisk Z, Sarrao J L, Thompson J D, Mandrus D, Hundley M F, Miglari A, Bucher B, Schlessinger Z, Aeppli G, Bucher E, DiTusa J F, Oglesby C S, Ott H-R, Canfield P C and Brown S E 1995 *Physica B* **206+207** 798
- [4] Takabatake T, Iga F, Yoshino T, Echizen Y, Katoh K, Kobayashi K, Higa M, Shimizu N, Bando Y, Nakamoto G, Fujii H, Izawa K, Suzuki T, Fujita T, Sera M, Hiroi M, Maezawa K, Mock S, von Löhneysen H, Brückl A, Neumaier K and Andres K 1998 *J. Magn. Magn. Mater.* **177–181** 277
- [5] Hundley M F, Canfield P C, Thompson J D, Fisk Z and Lawrence J M 1990 *Phys. Rev. B* **42** 6842
- [6] Malik S K, Menon L, Ghosh K and Ramakrishnan S 1995 *Phys. Rev. B* **51** 399
- [7] Sereni J G 1991 *Handbook on the Physics and Chemistry of Rare Earths* vol 15, ed K A Gschneidner Jr and L Eyring (Amsterdam: Elsevier Science) ch 98
- [8] Bickers N E, Cox D L and Wilkins J W 1985 *Phys. Rev. Lett.* **54** 230
- [9] Malik S K and Adroja D T 1991 *Phys. Rev. B* **43** 6277
- [10] Sales B C and Wohlleben D K 1975 *Phys. Rev. Lett.* **35** 1240
- [11] Rajan V T 1983 *Phys. Rev. Lett.* **51** 308
- [12] Batlogg B, Ott H R, Kaldis E, Thöni W and Wachter P 1979 *Phys. Rev. B* **19** 247
- [13] Lassailly Y, Vettier C, Holtzberg F, Benoit A and Flouquet J 1984 *Solid State Commun.* **52** 717
- [14] Fujii H, Kawanaka H, Takabatake T, Kurisu M, Yamaguchi Y, Sakurai J, Fujiwara H, Fujita T and Oguro I 1989 *J. Phys. Soc. Japan* **58** 2495
- [15] Nakotte H, Dilley N R, Torikachvili M S, Bordallo H N, Maple M B, Chang S, Christianson A, Schultz A J, Majkrzak C F and Shirane G 1999 *Physica B* **259–261** 280
- [16] Takabatake T, Nakamoto G, Yoshino T, Fujii H, Izawa K, Nishigori S, Goshima H, Suzuki T, Fujita T, Maezawa K, Hiraoka T, Okayama Y, Oguro I, Menovsky A A, Neumaier K, Brückl A and Andres K 1996 *Physica B* **223+224** 413
- [17] Takabatake T, Teshima F, Fujii H, Nishigori S, Suzuki T, Fujita T, Yamaguchi Y, Sakurai J and Jaccard D 1990 *Phys. Rev. B* **41** 9607
- [18] Takabatake T, Nagasawa M, Fujii H, Kido G, Nohara M, Nishigori S, Suzuki T, Fujita T, Helfrich R, Ahlheim U, Fraas K, Geibel C and Steglich F 1992 *Phys. Rev. B* **45** 5740
- [19] Coleman P, Miranda E and Tsvetlik A 1993 *Physica B* **186–188** 362
- [20] Aoki Y, Suzuki T, Fujita T, Kawanaka H, Takabatake T and Fujii H 1990 *J. Magn. Magn. Mater.* **90+91** 496
- [21] Aoki Y, Suzuki T, Fujita T, Kawanaka H, Takabatake T and Fujii H 1993 *Phys. Rev. B* **47** 15 060
- [22] Menon L and Malik S K 1997 *Phys. Rev. B* **55** 14 100
- [23] Malik S K, Menon L, Pecharsky V K and Gschneidner K A Jr 1997 *Phys. Rev. B* **55** 11 471

- [24] Hundley M F, Lacerda A, Canfield P C, Thompson J D and Fisk Z 1993 *Physica B* **186–188** 425
- [25] Ekino T, Takabatake T and Fujii H 1997 *Physica B* **230–232** 635
- [26] Sugiyama K, Iga F, Kasaya M, Kasuya T and Date M 1988 *J. Phys. Soc. Japan* **57** 3946
- [27] Jaime M, Movshovich R, Stewart G R, Beyermann W P, Berisso M G, Hundley M F, Canfield P C and Sarrao J L 2000 *Nature* **405** 160
- [28] Saso T and Itoh M 1996 *Phys. Rev. B* **53** 6877
- [29] Menon L, du Plessis P de V and Strydom A M 1998 *Solid State Commun.* **106** 519
- [30] Mirambet F, Chevalier B, Fournès L, Gravereau P and Etourneau J 1994 *J. Alloys Compounds* **203** 29
- [31] Du Plessis P de V, Strydom A M and Tran V H 1999 *Solid State Commun.* **112** 391
- [32] Béal-Monod M T and Lawrence J M 1980 *Phys. Rev. B* **21** 5400
- [33] Kaczorowski D, Rogl P and Hiebl K 1996 *Phys. Rev. B* **54** 9891
- [34] Lawrence J M, Riseborough P S and Parks R D 1981 *Rep. Prog. Phys.* **44** 1
- [35] Evans S M M and Gehring G A 1989 *J. Phys.: Condens. Matter* **1** 10487
- [36] Iga F, Kasaya M, Suzuki H, Okayama Y, Takahashi H and Mori N 1993 *Physica B* **186–188** 419
- [37] Iga F, Shimizu N and Takabatake T 1998 *J. Magn. Magn. Mater.* **177–181** 337
- [38] Yoshii S, Kasaya M, Takahashi H and Mori N 1996 *Physica B* **223–224** 421
- [39] Hiraoka T, Kinoshita E, Takabatake T, Tanaka H and Fujii H 1994 *Physica B* **199–200** 440
- [40] Cooley J C, Aronson M C and Canfield P C 1997 *Phys. Rev. B* **55** 7533
- [41] Wachter P, Marabelli F and Bucher B 1991 *Phys. Rev. B* **43** 11 136
- [42] Ichas V, Griveau J C, Rebizant J and Spirlet J C 2001 *Phys. Rev.* **63** 45 109
- [43] Krishna-murthy H R, Wilkins J W and Wilson K G 1980 *Phys. Rev. B* **21** 1003
Krishna-murthy H R, Wilkins J W and Wilson K G 1980 *Phys. Rev. B* **21** 1044
- [44] Sakai O, Shimizu Y and Kasuya T 1989 *J. Phys. Soc. Japan* **58** 3666
- [45] Sakai O, Shimizu Y, Takayama R and Kasuya T 1990 *Physica B* **163** 695
- [46] Costi T A, Hewson A C and Zlatić V 1994 *J. Phys.: Condens. Matter* **6** 2519
- [47] Oppeneer P M, Kraft T and Brooks M S S 2000 *Phys. Rev. B* **61** 12 825